

Ordering in Two-Dimensional Ising Models with Competing Interactions

Gennady Y. Chitov and Claudius Gros

Department 7.1-Theoretical Physics, University of Saarland, Saarbrücken D-66041, Germany

(Dated: May 22, 2019)

We study the 2D Ising Model on a square lattice with additional non-equal diagonal next-nearest neighbor interactions. The cases of classical and quantum (transverse) models are considered. Possible phases and their locations in the space of three Ising couplings are analyzed. In particular, incommensurate phases, occurring only at non-equal diagonal couplings, are predicted. In a particular region of interactions, corresponding to the Ising model's super-antiferromagnetic (SAF) ground state, we also consider a spin-pseudospin model comprised of the quantum Ising model coupled to XY spin chains. The spin-pseudospin model's spin-SAF transition into the phase with co-existent the SAF Ising (pseudospin) long-range order and the spin gap, has the properties analogous to the reported earlier by us (cond-mat/0310494) for a simpler coupled model. Along with destruction of the quantum critical point of the transverse Ising model, the phase diagram of the spin-pseudospin model can also demonstrate a re-entrance. A detailed study of the latter is presented. The mechanism of the re-entrance, due to interplay of interactions in the coupled model, and the conditions of its appearance are established.

PACS numbers: 71.10.Fd, 71.10.Hf, 75.30.Et, 64.60.-i

I. INTRODUCTION

The role of competing interactions in ordering is a fascinating problem of condensed matter physics. One of the most canonical examples of such systems are frustrated Ising models which demonstrate a plethora of critical properties, far from being exhaustively studied. (For a review see Ref.[1].) The frustrations² can be either geometrical, like, e.g., in the Ising model on a triangular lattice, or they can be brought about by the next-nearest neighbor (nnn) interactions. Competing interactions (frustrations) can, e.g., result in new phases, change the Ising universality class, or even destroy the order at all. Another interesting aspect of the criticality in frustrated Ising models is an appearance of Quantum Critical Point(s) (QCP) at special frustration points of model's high degeneracy, and related quantum phase transitions.

Inclusion of a transverse field (Ω) brings a new scale into the game, which makes the critical behavior even more complicated. The Ising model with $\Omega = 0$ and $\Omega \neq 0$ are also often called classical and quantum, respectively. For a review on the Ising Models in Transverse Field (IMTF) see Ref.[3]. Most of the studies on the frustrated quantum Ising models are restricted to their ground states properties, where the mapping of the d -dimensional quantum model at $T = 0$ onto its $(d + 1)$ -dimensional classical counterpart helps to analyze the ground state phase diagram of the former. For nnn 2D models we are interested, there was a considerable effort on the quantum ANNNI model, reviewed in Ref.[3]. The studies on some other 2D frustrated transverse Ising models have appeared only recently.^{4,5}

Our interest to the nn and nnn Ising model with $\Omega = 0$ and $\Omega \neq 0$ comes from the earlier work on a 2D IMTF coupled to the spin chains.⁶ This kind of coupled so-called spin-pseudospin (or spin-orbital) models appear in analyses of the phase transition in the quasi-2D quarter-filled ladder compound NaV_2O_5 , which has inspired a great experimental and theoretical effort in recent years. (For a review see Ref.[7].) Going deeper into analysis, we came to realize that the Ising sector of the problem is in fact the 2D transverse nn and nnn Ising model on a square lattice. It turns out that even its classical counterpart ($\Omega = 0$) was studied only for the case of the equal nnn couplings $J_1 = J_2$.¹ (The elementary plaquette of this lattice with the notations for couplings is shown in Fig. 1.) To the best of our knowledge, this 2D nn and nnn Ising model in transverse field is a complete *terra incognita* even at $J_1 = J_2$.

So, as the first step, we find the ground state phase diagram of the classical ($\Omega = 0$) Ising model at arbitrary couplings J_\square, J_1, J_2 . Along with the three ordered phases found earlier by Fan and Wu⁸ for the case $J_1 = J_2$ —ferromagnetic (FM), antiferromagnetic (AF), and super-antiferromagnetic (SAF)—the model has a fourth phase which can occur if $\text{sign}(J_1/J_2) = -1$. We call it super-ferro-antiferromagnetic (SFAF).⁹ From simple mean-field arguments we predict also the existence of an incommensurate (IC) phase at $T > 0$ in this model. The 2D IC phase is also called floating. Similar phase is known for the well-studied 2D ANNNI model.^{1,10,11} We present a qualitative temperature phase diagram for the regions of the coupling space where the IC phase is located. Note that the three phases – SAF, SFAF, IC – can occur only in the presence of competing interactions in the Ising model, and the latter two occur only if $J_1 \neq J_2$.

This analysis of the classical Ising model lays the grounds for venturing into its study in a presence of transverse field. The role of transverse field is subtle. A more straightforward aspect is that its increase can eventually destroy

the ordered state of the classical model, i.e., the appearance of a QCP. This is similar to the well-understood quantum nn Ising model. Another particularly interesting aspect in the role of transverse field is that it can lift the degeneracy of the ground state and create new temperature phases in a highly frustrated model, like, e.g., the antiferromagnetic isotropic triangular Ising model,^{4,5} which is disordered at any $T > 0$ when $\Omega = 0$.

The behavior of the systems with infinitely degenerate ground states (with or without a finite ground-state entropy per spin) can be quite complicated in the presence of transverse field. It lies beyond the scope of the present work, and definitely cannot be understood from the mean-field analysis we apply in this study. For the nn and nnn Ising model we only identify the lines (planes) in the space of couplings (J_{\square}, J_1, J_2) where the model is highly degenerate, and in their neighborhood we expect some new exotic phases generated by $\Omega \neq 0$ to appear.

From the mapping of the nn and nnn IMTF at $T = 0$ to its classical 3D counterpart we find the (mean-field) ground-state phase boundaries of the quantum model in the coupling space (J_{\square}, J_1, J_2) . In particular, it follows from our analysis that in the presence of transverse field the IC ground-state phase can penetrate into some parts of the FM, AF, SAF regions of the classical model ($\Omega = 0$).

Finally, we consider the nn and nnn IMTF coupled to the XY spin chains. In the case of this coupled model we restrict our analysis to the SAF region of the couplings (J_{\square}, J_1, J_2) , away from the highly degenerate manifolds and from the sectors where the IC can intervene. In this “safe” region the nn and nnn IMTF has a simple two-phase (disordered-SAF) diagram with a QCP, similar to that of the transverse nn Ising model. Since the SAF state is only four-fold degenerate, the mean-field predictions can be trusted.

This coupled spin-pseudospin model appears in the context of the compound NaV_2O_5 . Its 2D lattice of coupled ladders can be mapped onto an effective square lattice. The Ising sector of this model is given by the Hamiltonian of the nn and nnn IMTF, and the Ising variables (called pseudospins for this case) correspond physically to the charge degrees of freedom of NaV_2O_5 . A particular feature of the phase transition in this compound is a simultaneous appearance of charge order and spin gap. For the first time, we identify the 2D long-range charge order in NaV_2O_5 as the SAF phase. From simple geometric considerations of the NaV_2O_5 -lattice immediately follows that the Coulomb-generated antiferromagnetic couplings (J_{\square}, J_1, J_2) indeed lie in the SAF ground-state region of the nn and nnn Ising model’s phase diagram.

The mean-field equations for the coupled model with some minor modifications are the same as we have obtained earlier.⁶ A striking feature of the coupled model is that it *always* orders from the charge-disordered spin-gapless state into the phase of co-existent SAF charge order and spin gap. We call this the spin-SAF transition. By *always* we mean that the critical temperature of the spin-SAF transition is non-zero for all Ising couplings within the whole considered SAF region. In other words, the QCP of the IMTF is destroyed, and this is due to the nnn spin-pseudospin coupling, linear over pseudospin. This property of the spin-SAF transition and the parameters of the spin-SAF phase on the disordered side of the IMTF QCP were studied earlier in detail,⁶ so in this work we only reinstate some points in the context of the present model.

The other qualitative feature of the coupled model’s phase diagram is re-entrance, which was not well understood in our earlier work.⁶ Now we carry out an analytical study of the re-entrance and establish the conditions when it can occur. This analysis allows us to understand the mechanism of re-entrance in detail. Qualitatively, the re-entrance is due to competing interactions in the coupled model.

The rest of the paper is organized as follows. Section II contains our results on the ordering in the 2D nn and nnn Ising model at $\Omega = 0$ and $\Omega \neq 0$. The results on the phase transition in the 2D nn and nnn IMTF coupled to the XY spin chains are presented in Section III. The results are summarized and discussed in the final Section IV.

II. 2D NEAREST- AND NEXT-NEAREST-NEIGHBOR ISING MODEL

We consider the 2D Ising Model on a square lattice with nearest- and next-nearest neighbor interactions (see Fig. 1). Its Hamiltonian reads

$$H = \frac{1}{2} \sum_{\langle i,j \rangle} J_{\square} \mathcal{T}_i^x \mathcal{T}_j^x + \frac{1}{2} \sum_{\langle\langle \mathbf{k},\mathbf{l} \rangle\rangle} J_{\mathbf{kl}} \mathcal{T}_{\mathbf{k}}^x \mathcal{T}_{\mathbf{l}}^x \quad (1)$$

where the bold variables denote lattice vectors, the first [second] sum includes only nearest neighbors (nn) [next-nearest neighbors (nnn)] of the lattice, respectively. Spins along the sides of an elementary plaquette interact via the nn Ising coupling J_{\square} , while spins along plaquette’s diagonals interact via the nnn Ising couplings $J_{\mathbf{kl}} = J_{1,2}$. The way we defined the Hamiltonian corresponds to antiferromagnetic couplings for $J_{\ddagger} > 0$ and ferromagnetic for $J_{\ddagger} < 0$.

A. Ground state phases

There is no exact solution of the 2D nn and nnn Ising model. Its possible ordered phases and critical properties have been studied within various approaches for the case of equal diagonal couplings $J_1 = J_2$ (For a review and references on the original literature, see Ref.[1].) We will consider arbitrary Ising couplings (J_1, J_2, J_\square) , so the model (1) can be either frustrated or not.² The phase diagram of the ground states can be found from the energy arguments, as was first done by Fan and Wu for the case $J_1 = J_2$.⁸ (Their phase diagram is shown in Fig. 3c) From direct counting of the ground-state energies of possible spin arrangements, we construct the phase diagram for $J_1 \neq J_2$. Along with the possible ordered phases found by Fan and Wu– ferromagnetic (FM), antiferromagnetic (AF), and super-antiferromagnetic (SAF)– there is a fourth phase which can occur if J_1 and J_2 have opposite signs. The SAF phase was named like that because it can be viewed as the one created by two superimposed antiferromagnetic lattices (one lattice of circled sites and another of squared sites in Fig. 1). In the SAF state two plaquette’s J_\square -bonds are frustrated. The energy of this state is four-fold degenerate, since each of those lattices can be flipped independently. Or, to put it differently, along with the SAF state shown in Fig. 1 where the spins are ordered ferromagnetically in horizontal chains (alternating from chain to chain), there is an equivalent state with the vertical ferromagnetic order.

The new fourth phase shown in Fig. 1 can be viewed as two superimposed lattices each of which is ordered ferromagnetically along one side (e.g., $J_2 < 0$) and antiferromagnetically along the other (e.g., $J_1 > 0$). So we will call it super-ferro-antiferromagnetic (SFAF).⁹ The SFAF state also has two frustrated plaquette bonds, and its energy is four-fold degenerate. However the ordering pattern shown in Fig. 1 only shifts by a lattice unit over flipping one of the lattices (circled or squared). The direction of the ferromagnetic order in the SFAF state is determined by the ferromagnetic diagonal.

The ground-state phases in the space (J_1, J_2, J_\square) are shown in Fig. 2. In order to facilitate perception of this picture, we also present in Figs. 3,4 several plane projections of the 3D Fig. 2. In the first quadrant $(J_1, J_2 > 0)$ in the region $J_1 + J_2 > |J_\square|$ lying between two frustration planes FP

$$J_1 + J_2 = |J_\square| : \quad \text{FP} \quad (2)$$

the ground state of the model is the SAF phase. Transition from the disordered paramagnetic (PM) phase into the SAF phase should occur at some finite critical temperature $T_c > 0$. From the same arguments as in the case $J_1 = J_2$,¹² (see also Ref.[13] for a more general symmetry analysis of the Ginzburg-Landau functional) we conclude that such (continuous) phase transition is non-universal, the critical indices continuously depend on the couplings J_\square, J_1, J_2 .

In the region $J_1 > J_\square$ of the fourth quadrant $(J_1 > 0, J_2 < 0)$ lying between the other pair of frustration planes FP’

$$J_1 = |J_\square| : \quad \text{FP}' \quad (3)$$

the ground state is the SFAF phase. As in the above case, the PM \rightarrow SFAF transition should be non-universal.

In the regions of the 3D coupling space lying above (beneath) the frustration planes FP and FP’, and above (beneath) the basal plane $J_\square = 0$ in the third quadrant, the ground state of the system is a usual AF (FM) phase, respectively. The phase transition PM \rightarrow AF (FM) belongs to the 2D Ising universality class. (The second quadrant $J_1 < 0, J_2 > 0$ not shown in Fig. 2, is obtained by a reflection over the plane $J_1 = J_2$.) In the AF (FM) state the number of frustrated (diagonal) bonds per plaquette is two in the first quadrant, one in the second and the fourth, and zero in the third.

On the frustration planes FP/FP’ the model is highly degenerate, and the critical temperature of the ordering into SAF/SFAF phases should vanish. We are not aware of studies of the ground state in these cases, and cannot say at the moment whether the system possesses some kind of a long-range order at zero temperature or not, except a rather trivial line $J_\square = J_1 = 0, J_2 < 0$ of the FP’ planes crossing where the model becomes a set of decoupled Ising chains, and four special lines on the FP planes where it becomes the exactly-solvable Isotropic Triangular Ising (ITI) model. The latter case will be discussed momentarily.

B. Exactly-solvable limits

In the 3D space (J_1, J_2, J_\square) beside the frustration planes FP and FP’, there are three special planes where one of the couplings is zero. These planes warrant separate analyses. These are the cases when the model (1) reduces to the exactly solvable cases.

Let us start with the upper part ($J_\square > 0$) of the SAF region

$$J_\square < J_1 + J_2 \quad (4)$$

On the SFAF-SAF boundary $J_2 = 0$ the model is equivalent to the anisotropic Ising model on a triangular lattice (ATI), for which exact results are available.^{14,15,16,17} From the results of Ref.[17] we infer that the antiferromagnetic ($J_\square, J_1 > 0$) ATI model with one strong bond $J_1 > J_\square$ is disordered at any non-zero temperature. It orders only at $T = 0$, i.e., it is Quantum Critical (QC). The highly degenerate ground state (however with a vanishing zero-temperature entropy per site) can be viewed as a 2D array of chains (along the strong bond J_1) which are antiferromagnetically ordered, and there are correlations between them. The oscillating (with a period of four lattice spacings) power-law decay of the spin-spin correlation function along J_\square -directions¹⁷ indicate on the preference of the ferromagnetic ordering along the “missing” diagonal J_2 . This resembles the SFAF state, however any couple of adjacent J_1 -chains is uncorrelated. We label this state occurring on two sectors of the J_1 (or J_2) = 0 planes as ATI (QC) on the phase diagram (Fig. 2). Note that since the critical behavior of the ATI model with two equal weak ferromagnetic bonds $|J_\square| < J_1$ is equivalent to the totally antiferromagnetic ATI model,¹⁷ the ATI (QC) state smoothly continues into the lower ($J_\square < 0$) part of the SFAF-SAF boundary.

The sectors $J_2 = 0, J_1 > 0$ (and $1 \leftrightarrow 2$) above the FP $J_1 + J_2 = J_\square$ correspond to the antiferromagnetic ATI model with one weak bond $J_1 < J_\square$. It is known¹⁷ to have only two phases and to order at finite temperature. $T_c(\text{PM} \rightarrow \text{AF})$ as a function of couplings can be found exactly. The sectors $J_2 = 0, J_1 < 0, J_\square > 0$ (and $1 \leftrightarrow 2$) correspond to the antiferromagnetic ATI model which is even not frustrated, and $T_c(\text{PM} \rightarrow \text{AF}) > 0$ at any $J_\square > 0$. The $\text{PM} \rightarrow \text{AF}$ transition in the ATI model belongs to the 2D Ising class. So, except the SFAF-SAF boundary, the ordered phase on the exactly-solvable “triangulation” planes J_1 (or J_2) = 0 is the same as the AF ground state in the interior in this region of the phase diagram.

The situation on the “triangulation” planes in the lower part ($J_\square < 0$) of the phase diagram is exactly analogous to the upper part, with an obvious replacement $\text{AF} \leftrightarrow \text{FM}$.

Note that the ground states change on the lines where the triangulation and frustration planes cross. To put it differently, these are the lines of quantum phase transitions. The AF (FM) phase disappears in the limit $J_1 \rightarrow |J_\square| - 0$ ($J_2 = 0$). Also, the zero-temperature AF in-chain order [ATI (QC)] described above disappears in the limit $J_1 \rightarrow |J_\square| + 0$ ($J_2 = 0$) as well. The ITI model $J_1 = J_\square$ is disordered at any non-zero temperature (indicated as ITI (QC) in Fig. 2). Its ground state, albeit having finite entropy per site, possesses periodical (with a period of three lattice spacings) long-range order.¹⁶

The basal plane $J_\square = 0$ in Fig. 2 corresponds to the case when Hamiltonian (1) represents two decoupled identical nn Ising models residing on two superimposed lattices (shown by circles and squares in Fig. 1). Diagonal couplings $J_{1,2}$ are the nn couplings of these Ising models. This is the only exactly-solvable limit (labelled by $2 \times 2\text{DI}$ in Fig. 2) within the SFAF (or SAF) region of the phase diagram. In this limit the $\text{PM} \rightarrow \text{SAF}$ (or SFAF) phase transition enters into the 2D Ising universality class.

C. Incommensurate (floating) phase

So far we have discussed the ground-state phases of the model and the critical behavior on the boundaries of these phases with the disordered phase, as well as on the special planes (lines). However, there is also a possibility that ordering into the ground-state phases of Fig. 2 happens not necessarily from the PM phase, but from some other one(s) occurring at non-zero temperature. A very simple analysis indicates that this indeed can take place in our model. Fourier-transforming the Hamiltonian (1) we obtain (we set the lattice spacing to unity)

$$H = \sum_{\mathbf{q}} J(\mathbf{q}) T^x(\mathbf{q}) T^x(-\mathbf{q}), \quad (5)$$

$$J(\mathbf{q}) = J_\square(\cos q_x + \cos q_y) + J_1 \cos(q_x - q_y) + J_2 \cos(q_x + q_y)$$

where \mathbf{q} runs within the first Brillouin zone $|q_{x,y}| \leq \pi$. At mean-field level, a minimum of $J(\mathbf{q})$ in \mathbf{q} -space defines the wave-vector \mathbf{q}_0 of the critical freezing mode $T^x(\mathbf{q}_0)$, i.e. the order parameter $\langle T_{\mathbf{m}}^x \rangle \propto \cos(\mathbf{q}_0 \mathbf{m} + \varphi)$ below a certain critical temperature T_c . In different regions (J_1, J_2, J_\square) of the ground-state phase diagram (Fig. 2) we find minimum at $\mathbf{q}^{\text{F/A}} = (0, 0)/(\pi, \pi)$ giving the FM/AF order parameter and two minima $\mathbf{q}_{1,2}^{\text{SAF}} = (\pi, 0)/(0, \pi)$ giving two components of the SAF order parameter. (The latter represent two possible ordering patterns of the SAF phase, or via some transformation can be related to magnetizations of the superimposed sublattices.¹²) The important point is that the positions of the *commensurate* (C) extrema \mathbf{q}^\sharp ($\sharp = \text{F, A, SAF}$) of $J(\mathbf{q})$ do not depend on couplings.

There are however two other pairs of extrema $\pm \mathbf{q}^{s,a}$ which exist if

$$|J_\square| < 2|J_1| \quad \text{and/or} \quad 2|J_2| \quad (6)$$

These extrema lie on the diagonal of the Brillouin zone. $\mathbf{q}^{s,a}$ are generically *incommensurate* (IC) and depend on

couplings as

$$q_x^s = q_y^s = \arccos\left(-\frac{J_\square}{2J_2}\right) \quad (7)$$

$$q_x^a = -q_y^a = \arccos\left(-\frac{J_\square}{2J_1}\right) \quad (8)$$

We show the positions of all extrema of $J(\mathbf{q})$ within the Brillouin zone in Fig. 5. In the SFAF ground-state region (e.g., in the fourth quadrant $J_1 > 0, J_2 < 0$ shown in Fig. 2) the pair of extrema $\pm\mathbf{q}^a$ (8) gives global minima of $J(\mathbf{q})$ (the other pair of solutions (8) $\pm\mathbf{q}^s$ when exists, corresponds to its maxima), and $|q_x^a| = |q_y^a| > \pi/2$. As we see, two IC modes $\pm\mathbf{q}^a$ could give components of the SFAF ground-state order parameter's wave vectors $\pm\mathbf{q}^{\text{SFAF}} = \pm(\pi/2, -\pi/2)$ only if $J_\square = 0$. (In the second quadrant of the SFAF region when $J_1 < 0, J_2 > 0$, the vectors \mathbf{q}^s and \mathbf{q}^a exchange their roles. Because of the $J_1 \leftrightarrow J_2$ symmetry, in the following we will always discuss the fourth quadrant for concreteness.)

The locus of the IC global minima does not coincide with the SFAF ground-state region, but overlaps with the neighboring FM, AF, and SAF phases. The minimum $J(\pm\mathbf{q}^a)$ is located between two planes $|J_\square| = 2J_1$ in the fourth quadrant, and in two regions of the $J_2 < J_1$ half of the first quadrant: (i) between $J_\square = +2J_1$ and $J_\square = +2\sqrt{J_1J_2}$; (ii) $+$ \mapsto $-$. The regions of the IC minima in the other half ($J_2 > J_1$) of the first quadrant (as in the second quadrant) are obtained from the described above by $J_1 \leftrightarrow J_2$, $\mathbf{q}^a \mapsto \mathbf{q}^s$. On the plane phase diagram shown in Fig. 4 this locus is restricted by the lines $y = 1/2$, $x = 1/2$, $y = 1/4x$, shown by the black dashed lines.

So we can conclude that at finite temperature the model possesses an IC phase and there is an IC-C phase transition where the IC wave vector \mathbf{q}^a locks into one of the (commensurate) ground-state phase vectors. As in 2D the IC phase has only an *algebraic* long-range order, it is called floating.¹⁰ The origin of the IC floating phase in our model is frustration (competing interactions). Such phase is well known from another example of frustrated Ising model, i.e., the ANNNI model which was intensively studied in the past.^{1,10,11} In that model the floating phase locks into the antiphase which has the wave vector $\mathbf{q} = (0, \pi/2)$. (The antiphase is analogue of our SFAF phase.) The ANNNI model also provides an example showing that the mean-field (minimization) analysis does not work well in defining boundaries between the floating and commensurate phases in 2D, and the extend of the IC phase is *less* than the mean field suggests.¹⁸

We will not attempt to locate exactly the phase boundaries at finite temperature in this study. Following Domany *et al*¹³ in the classification of ordered phases by the ratio (p , commensurability) of ordered structure's and lattice's periods in a given direction, we can label the phases as follows: F \mapsto 1×1 ; AF \mapsto 2×2 ; SAF \mapsto 1×2 (or 2×1); SFAF \mapsto 4×4 .¹⁹ From mapping of the 2D IC-C phase transition to the Kosterlitz-Thouless problem, it is established that there is no such (continuous) transition for commensurate phases with small $p^2 < 8$.^{10,20} From this result we conclude that the IC floating phase cannot "spill" beyond the SFAF ($p = 4$) ground-state region of the phase diagram, even if a naive analysis suggests that within the F, AF, and SAF regions there are some parts where it could be possible (see Fig. 4). The only high-temperature phase the latter three regions have a common border, is the disordered PM. Combining this with the exact critical properties of the model on the special planes discussed above, we end up with the finite-temperature phase diagram shown in Fig. 6. Since on the plane $J_\square = 0$ the model is just two decoupled Ising lattices, the floating phase is absent. Mean-field arguments suggest that the floating phase disappears exactly at $J_\square = 0$ giving rise to a Lifshitz point (L).

Note that the floating phase does not appear in the case of equal diagonal couplings $J_1 = J_2$ even at the mean-field level (see Fig. 4), which agrees with known more sophisticated analyses of this case.¹

D. The model in transverse field

Now we turn to the analysis of the nn and nnn Ising Hamiltonian H (1) in the presence of a transverse field. The total Hamiltonian of the Ising Model in Transverse Field (IMTF) reads

$$H_{\text{IMTF}} = H - \Omega \sum_{\mathbf{i}} \mathcal{T}_{\mathbf{i}}^z \quad (9)$$

The Ising operators are normalized to satisfy the spin algebra

$$[\mathcal{T}_{\mathbf{i}}^\alpha, \mathcal{T}_{\mathbf{j}}^\beta] = i\delta_{\mathbf{ij}}\epsilon_{\alpha\beta\gamma}\mathcal{T}_{\mathbf{i}}^\gamma \quad (10)$$

There is no exact solution of the 2D Ising model in a transverse field even for the case of nn couplings only ($J_1 = J_2 = 0$). The ground state phase diagram of the Hamiltonian (9) can be analyzed from the known mapping of the d -dimensional IMTF at zero temperature onto the $(d+1)$ -dimensional Ising model at a given (non-zero)

“temperature”.³ In our case the 2D nn and nnn IMTF maps onto the 3D Ising model comprised of the 2D layers (1) coupled *ferromagnetically* in the third (Trotter) direction with the coupling $J_T \propto -\ln \coth \Omega < 0$. For such (2+1)-dimensional model a mean-field analysis gives a qualitatively correct diagram of the *ground state* phases of the 2D IMTF.³ The new coupling J_T does not bring any additional frustration to the 2D nn and nnn model. Analysis of $J_3(q_x, q_y, q_T) = J_T \cos q_T + J(q_x, q_y)$ where $J(q_x, q_y)$ is given by (5), shows that J_T does not modify the domains of the global minima in the (J_1, J_2, J_\square) -space, adding only a trivial $q_T = 0$ component to the two-dimensional vectors \mathbf{q}^\sharp discussed above (cf. Fig. 5.) The temperature phase diagram of the 3D Ising model with the spectrum $J_3(q_x, q_y, q_T)$ (if we label the phases according to the in-plane ordering pattern defined by the 2D vectors \mathbf{q}^\sharp) looks similar to the one shown in Fig. 6, with one very important distinction: the abovementioned argument related to phase’s commensurability order p does not apply in 3D, so the IC region is not restricted to lie above the SFAF phase, but can spill into the neighboring regions of the (J_1, J_2, J_\square) -space. From the mean-field arguments, the IC region is given by the locus of the IC minima $J(\pm \mathbf{q}^{a/s})$ defined in the previous section. So, the IC phase instead of being locked between the special planes FP' and $J_2 = 0$ as shown in Fig. 6 (a) and (b), respectively, can spread up to the locus boundaries shown by the crosses. From the equivalence between the zero-temperature d -dimensional IMTF (quantum Ising) and the $(d+1)$ -dimensional classical Ising model, we infer that the ground-state phase diagram of the former on the plane $(\Omega/J, J_\sharp)$ should have the same structure as the described above (T, J_\sharp) diagram of the latter. So we expect the transverse field to generate the IC ground-state phase not only in the SFAF region of the the Ising coupling space, but also in the neighboring parts of the F, AF, and SAF regions. From minimization arguments the latter are restricted by the dashed lines on the plane diagram in Fig. 4 and by the crosses in Fig. 6.

From analogies with the ANNNI model, we rather expect this “IC region” to be filled with infinitely many commensurate phases of different type,^{10,11} but detailed analysis of this question, as well as the full *finite-temperature* phase diagram of the model with a transverse field need a separate study.

In the rest of the paper we will be particularly interested in the SAF region of the coupling space, and restrict ourselves to the couplings

$$J_\square^2 < 4J_1 J_2, \quad (J_1, J_2) > 0 \quad (11)$$

According to Fig. 4, it means that we choose the couplings to lie above the hyperbole $y = 1/4x$. The first condition in (11) ensures that the couplings lie in the region where $\mathbf{q}_{1,2}^{\text{SAF}} = (0, \pi)/(\pi, 0)$ provide a global minimum of model’s spectrum, so the phase with the IC solutions $\mathbf{q}^{a/s}$ does not intervene. The second in the above conditions stipulates that even if $J_\square = 0$ we stay away from the planes where our model becomes the triangular Ising. In that model a transverse field can generate exotic temperature phases. Such phases were found in the particular case of the isotropic (antiferromagnetic) transverse triangular Ising model.^{4,5,21}

From the mapping between the quantum and classical Ising models we conclude that at zero temperature our IMTF with (11) possesses a single Quantum Critical Point (QCP) [i.e., a value of $\Omega_{\text{cr}}/J_\sharp$] which separates the SAF and PM phases. It is also known that for the IMTF ($d \geq 2$) the mean-field approximation gives a qualitatively correct phase diagram, albeit with some numerical deviations from more accurate results.³ In our case the mean-field predicts a two-phase (PM,SAF) diagram with the critical temperature T_c of the second-order phase transition between these phases going smoothly from the QCP $T_c(\Omega_{\text{cr}}/J_\sharp) = 0$ to the $T_c(0) > 0$ of the model without transverse field (it is shown by the dashed line in Fig. 8, where $g \equiv (J_1 + J_2)/\Omega$). This is the phase diagram of the IMTF (1,9) with the constants satisfying (11) before we couple it to other degrees of freedom.

III. COUPLED SPIN-PSEUDOSPIN MODEL

A. Hamiltonian

Now we turn to the analysis of the IMTF (1,9) coupled to the independent quantum spins (\mathbf{S}) residing on the same sites of the lattice as the Ising spins do. The latter we will call pseudospins from now on. We assume the spins to be coupled with the XY -exchange along the J_1 -diagonals (cf. Fig. 1) only, so they form chains along that direction. Each pseudospin \mathcal{T} is coupled to its nnn spin \mathbf{S} along the J_2 -diagonal.

Models of this type appear in analyses of the quarter-filled ladder compound NaV_2O_5 , and pseudospins represent its charge degrees of freedom. See Ref.[7] for a review. The Hamiltonian of this compound can be mapped onto a spin-orbital (pseudospin) model,²² with spins and pseudospins residing on the same ladder’s rung.^{23,24,25} These ladders form a 2D lattice. The long-range order attributed to $\langle T_1^x \rangle \neq 0$, is physically related to the charge disproportionation between left/right sites on a rung occurring below a certain critical temperature. This system can be analyzed on the effective triangular lattice shown in Fig. 7a by solid lines.^{23,25} Note however, that in the case of NaV_2O_5 the Ising couplings, generated by Coulomb repulsion, are antiferromagnetic, and $J_1 > J_\square$. Since the triangular Ising model

with one strong side is disordered, one needs an extra coupling (J_2 -diagonal) to stabilize the observed SAF long-range order. In our related earlier study⁶ we explicitly took into account J_1 , while the other diagonal J_2 was effectively generated via the spin-pseudospin coupling.²⁶

In this work we take into account the Ising couplings J_\square, J_1, J_2 between neighboring sites of the effective lattice, as shown in Fig. 7a. Then such effective lattice can be mapped onto the square lattice shown in Fig. 7b with the nn and nnn Ising couplings. For the case relevant to NaV_2O_5 all $J_\# > 0$, so the model is frustrated. As follows from geometry of the original NaV_2O_5 lattice, J_2 is the weak diagonal and J_1 is the largest coupling:

$$J_2 < J_\square < J_1 \quad (12)$$

We assume J_\square to be small enough not only to lie beneath the frustration plane (2), but to satisfy a more stringent condition (11). Then according to the above analysis, the IMTF with these couplings has a two-phase (PE-SAF) diagram with a QCP.²⁷ Note also that in the literature on NaV_2O_5 its charge order is called the ‘‘zig-zag phase’’, what characterizes the antiferroelectric order in a *single ladder* only. In fact, the *two-dimensional long-range charge order* in NaV_2O_5 is SAF.

In the following we will work with dimensionless Hamiltonians $\mathcal{H} = H/\Omega$ and dimensionless temperature $T \rightarrow T/\Omega$. With the site labelling shown in Fig. 7, the dimensionless IMTF Hamiltonian is:

$$\mathcal{H}_{\text{IMTF}} = - \sum_{m,n} \mathcal{T}_{mn}^z + \frac{1}{2} \sum_{m,n} \left[g_\square \left(\mathcal{T}_{mn}^x \mathcal{T}_{m+1,n+1}^x + \mathcal{T}_{mn}^x \mathcal{T}_{m+1,n}^x \right) + g_1 \mathcal{T}_{mn}^x \mathcal{T}_{m,n+1}^x + g_2 \mathcal{T}_{mn}^x \mathcal{T}_{m+2,n+1}^x \right] \quad (13)$$

where we introduced the dimensionless Ising couplings $g_\# \equiv J_\#/\Omega$. As we infer from our previous work on a simpler version of the IMTF Hamiltonian,⁶ there are two spin-pseudospin interaction terms resulting in two qualitatively distinct aspects of the spin-pseudospin model’s critical properties: the inter-ladder spin-pseudospin interaction $\propto \varepsilon$, and the in-ladder spin-pseudospin interaction $\propto \lambda$. The former, in terms of the equivalent square lattice, linear over difference of the charge displacement operators \mathcal{T}^x on the nnn sites along the weak J_2 -diagonal, is responsible for the simultaneous appearance of the SAF order and the spin gap, as well as for the destruction of the IMTF QCP.²⁸ The latter, proportional to the product of the nnn charge operators along the J_1 -diagonal, is responsible for the re-entrance. With these terms, along with the usual Heisenberg exchange term $\propto J$, the total effective dimensionless Hamiltonian reads:

$$\mathcal{H} = \mathcal{H}_{\text{IMTF}} + \sum_{m,n} \mathbf{S}_{mn} \mathbf{S}_{m,n+1} \left[J + \lambda \mathcal{T}_{mn}^z \mathcal{T}_{m,n+1}^z + \varepsilon (\mathcal{T}_{m+1,n+1}^x - \mathcal{T}_{m-1,n}^x) \right], \quad (14)$$

The dimensionless couplings (J, λ, ε) in the Hamiltonian (14) are positive, and the spin operators satisfy the same algebra (10) as the pseudospins (while S and \mathcal{T} commute). The sums above run through $1 \leq m \leq \mathcal{M}$ and $1 \leq n \leq \mathcal{N}$. For brevity we use the notation $D_{mn} \equiv \mathbf{S}_{mn} \mathbf{S}_{m,n+1}$. In the present study we consider the model with the XY spin-spin interaction, i.e.,

$$D_{mn} = S_{mn}^x S_{m,n+1}^x + S_{mn}^y S_{m,n+1}^y \quad (15)$$

The range of the model’s parameters under consideration will be restricted to the cases

$$(J, \lambda) \lesssim g_1, \quad \varepsilon \lesssim \max\{J, \lambda\} \quad (16)$$

B. Spin-SAF phase transition

We treat the Hamiltonian (14) following conventional wisdom of molecular-field approximations (MFA).²⁹ In the present version of MFA the pseudospins are decoupled and averaged with the density matrix $\rho^\mathcal{T} \propto \exp(-\beta \mathbf{h}_{mn} \mathcal{T}_{mn})$, where \mathbf{h}_{mn} is the Weiss (molecular) field \mathbf{h}_{mn} , while the spin sector is treated exactly via a Jordan-Wigner transformation. The details are presented in Ref.[6]. Similar to the pure IMTF with couplings (11) we assume the possibility of the SAF order in the coupled model (14). So we take the following ansatz for the Ising pseudospin averages (i.e., the charge ordering parameters in terms of the real physical quantities)

$$\langle \mathcal{T}_{mn}^z \rangle = m_z \quad (17)$$

$$\langle \mathcal{T}_{mn}^x \rangle = (-1)^{m+n} m_x \quad (18)$$

It is easy to see from the Hamiltonian (14) that ansatz (18) creates a dimerization in the spin sector, therefore a natural assumption for the dimerization operator average is

$$\langle D_{mn} \rangle = -[t + (-1)^{m+n} \delta] \quad (19)$$

With the new coupling

$$g \equiv g_1 + g_2 \quad (20)$$

the molecular-field equations and all the results for the PE-SAF phase transition presented in Ref.[6] for the case $g_2 = g_\square = 0$ (i.e., $g = g_1$), apply here. Some of those formulas and results we reproduce in this paper in order to make it more self-contained, and for the use in what follows as well.

The average quantities are determined by the system of four coupled equations

$$m_z = \frac{1}{2} \frac{1 + 2\lambda t m_z}{\mathfrak{h}} \tanh \frac{\beta \mathfrak{h}}{2} \quad (21a)$$

$$m_x = \frac{m_x}{2} \frac{g + 2\varepsilon \eta}{\mathfrak{h}} \tanh \frac{\beta \mathfrak{h}}{2} \quad (21b)$$

$$t = \frac{1}{\pi} \int_0^{\frac{\pi}{2}} d\varphi \frac{\cos^2 \varphi}{\xi(\varphi)} \tanh \tilde{\beta} \xi(\varphi) \equiv \frac{1}{\pi} t_n(\Delta, \tilde{\beta}) \quad (21c)$$

$$\eta = \frac{\Delta}{\pi m_x} \int_0^{\frac{\pi}{2}} d\varphi \frac{\sin^2 \varphi}{\xi(\varphi)} \tanh \tilde{\beta} \xi(\varphi) \equiv \frac{\Delta}{\pi m_x} \eta_n(\Delta, \tilde{\beta}) \quad (21d)$$

where $\mathfrak{h} = \sqrt{h_x^2 + h_z^2}$ is the absolute value of the Ising molecular field

$$h_z = 1 + 2\lambda t m_z \quad (22a)$$

$$h_x = g m_x + 2\varepsilon \delta \quad (22b)$$

The other auxiliary parameters are defined as follows:

$$\delta \equiv m_x \eta \quad (23a)$$

$$\xi(\varphi) \equiv \sqrt{\cos^2 \varphi + \Delta^2 \sin^2 \varphi} \quad (23b)$$

$$\Delta \equiv \frac{2\varepsilon m_x}{J + \lambda m_z^2} \quad (23c)$$

$$\tilde{\beta} \equiv \frac{\beta}{2} (J + \lambda m_z^2) \quad (23d)$$

Below a certain critical temperature T_c the coupled model undergoes a phase transition from the disordered PE phase. Since the results for this transition obtained in Ref.[6] are straightforwardly applied here with a modification to the new coupling g (20), we will only shortly recapitulate the main properties of this transition. It is of the second kind, with the thermodynamic behavior of the physical quantities as the Landau theory of phase transitions predicts.⁶ With the spin-pseudospin (charge) coupling ε present in the Hamiltonian (14), the SAF charge order $m_x \neq 0$ below T_c is always accompanied by the spin gap $\Delta_{\text{SG}} = 2\varepsilon m_x$. By the analogy with the spin-Peierls transition, when the Peierls phonon instability (freezing) creates the spin gap, it is natural to call this type of transition with a simultaneous generation of the spin gap and the SAF charge order, the *spin-super-antiferroelectric (spin-SAF)* transition.

The behavior of $T_c(g)$ in the coupled model (14) shows two new striking features comparatively to the pure IMTF: re-entrance and destruction of the QCP.⁶ In the absence of the spin-charge coupling ε , the model (14) has a QCP at

$$g_\lambda \equiv 2 \left(1 + \frac{\lambda}{\pi} \right), \quad (24)$$

where T_c vanishes (see Fig. 8). Note that this QCP is renormalized by coupling λ comparatively to the QCP of the pure IMTF $g = 2$. The coupling ε , responsible for the spin gap generation, also destroys the QCP, resulting in the exponential behavior of T_c in the region of Ising's coupling $g < g_\lambda$ (BCS regime) This constitutes an important feedback from the spins on the charge degrees of freedom, allowing an ordering in the coupled model, which would have been disordered at any temperature if $\varepsilon = 0$. Approximate analytical solutions for $T_c(g)$ found in the regimes of strong Ising couplings and the BCS- are:⁶

$$T_c \approx \begin{cases} \frac{g}{4}, & g \gg g_\lambda \\ \frac{\mathbb{A} \tilde{J}}{2} \exp\left[-\frac{\pi \tilde{J}}{4\varepsilon^2} (g_\lambda - g)\right], & \text{BCS regime} \end{cases} \quad (25)$$

where $\mathbb{A} \equiv \frac{8}{\pi e^{1-\gamma}} \approx 1.6685$, $\gamma \approx 0.5772$ is Euler's constant, and

$$\tilde{J} \equiv J + \frac{\lambda}{4} \quad (26)$$

The boundary where the low-temperature BCS regime sets in and the related formulas are applicable, is given approximately by the condition

$$\text{BCS regime : } g < g_\lambda + \frac{4\varepsilon^2}{\pi\tilde{J}} \quad (27)$$

The BCS regime has many analogies with the standard theory of superconductivity, apart from the exponential dependence of T_c on couplings. In particular, several physical quantities (order parameter, BCS ratio, specific heat jump) manifest certain “universal” behavior near T_c , similar to that known from the BCS theory.⁶

Another particularity of the $T_c(g)$, found earlier in our related work⁶ from the numerical solution of Eqs.(21), is the re-entrance in the intermediate regime $g \sim g_\lambda$. The re-entrance occurs in the coupled model with the QCP ($\varepsilon = 0$), while when $\varepsilon \neq 0$ the critical temperature can even manifest a double re-entrant behavior before it reaches the BCS regime (see Fig. 8).

A detailed analysis of the coupled model in the regime of re-entrance was not done previously.⁶ We will address this in the next subsection, mainly analytically, in order to get more insight on the underlying physics, and, in particular, to establish conditions for model’s couplings when the re-entrance occurs.

C. Re-entrance

Let us first reproduce some earlier formulas⁶ for reader’s convenience. At $T \leq T_c$ one equation from the pair (21a,b) can be written in a more convenient form

$$m_z^{-1} = g + \frac{4\varepsilon^2}{\pi(J + \lambda m_z^2)} \eta_n - \frac{2\lambda}{\pi} t_n, \quad T \leq T_c \quad (28)$$

At $T = T_c$ we have Eqs.(21a) as

$$m_z = \frac{1}{2} \tanh \frac{\beta_c}{2} \left(1 + \frac{2\lambda m_z t_n}{\pi} \right), \quad (29)$$

and parameters t_n, η_n are given by Eqs.(21c,d) with $\Delta = 0$. The latter two functions have the following expansions:⁶

$$t_n(0, x) \approx \begin{cases} \frac{\pi}{4} x (1 - \frac{1}{4} x^2) + \mathcal{O}(x^5), & x < 1 \\ 1 - \frac{\pi^2}{24} \frac{1}{x^2} + \mathcal{O}(\frac{1}{x^4}), & x > 1 \end{cases} \quad (30)$$

and

$$\eta_n(0, x) \approx \begin{cases} \frac{\pi}{4} x (1 - \frac{1}{12} x^2) + \mathcal{O}(x^5), & x < 1 \\ \ln \Delta x + \frac{\pi^2}{48} \frac{1}{x^2} + \mathcal{O}(\frac{1}{x^4}), & x > 1 \end{cases} \quad (31)$$

1. Case $\varepsilon = 0$; re-entrance with QCP

As one can easily see from Eqs.(28,29) there is no re-entrance when $\lambda = 0$. This is a well-known fact for the pure IMTF, as on the mean-field level, as well as beyond MFA.^{3,29}

In order to study the re-entrance analytically, and in particular, to establish whether there is some minimal value of λ when it appears, we should distinguish between two asymptotic regimes of the mean-field equations. Let us first consider the regime (it can occur only if $\tilde{J} < 1$) when ($T_c \equiv 1/\beta_c$)

$$\frac{1}{2} \tilde{J} < T_c < \frac{1}{2} \quad (32)$$

(Note that in all regimes of couplings the re-entrance occurs at $T_c < \frac{1}{2}$). By carrying out the leading-term expansions of the functions t_n, \tanh entering Eqs.(28,29), we obtain the approximate equation

$$g = 2 + 4e^{-1/T_c} + \frac{\lambda\tilde{J}}{4T_c} \quad (33)$$

for a single-valued function $g(T_c)$. The non-monotonic (i.e., re-entrant) behavior of $T_c(g)$ is related to the existence of an extremum of $g(T_c)$. The coupling g_{\min} which defines the minimal value of g for the order in m_x being possible (in the pure IMTF with $\lambda = 0$ this was the QCP), and in the same time the left border of the re-entrant region

$$g_{\min} < g < g_\lambda, \quad (34)$$

is defined from the minimum of the function $g(T_c)$ (33). One finds that this point corresponds to the critical temperature

$$T_* = \ln^{-1} \kappa_o, \quad \kappa_o \equiv \frac{16}{\lambda \tilde{J}} \quad (35)$$

for which

$$g_{\min} \approx 2 + \frac{4}{\kappa_o} (1 + \ln \kappa_o) \quad (36)$$

The consistency of the solution (35) with (32) implies the condition

$$2 < \ln \kappa_o < \frac{2}{\tilde{J}}, \quad (37)$$

The other regime corresponds to the case when

$$T_c < \min\{1/2, \tilde{J}/2\} \quad (38)$$

Proceeding in the same way as above, we obtain the approximation

$$g = g_\lambda + 4e^{-g_\lambda/2T_c} - \frac{\lambda\pi}{3\tilde{J}^2} T_c^2 \quad (39)$$

for $g(T_c)$ in this case.

Let us point out that the conditions (32,38) determine two different regimes ($x < 1$ or $x > 1$) of the asymptotics (30,31) we apply in order to obtain $g(T_c)$ as (33) or (39). So if $\tilde{J} < 1$ there are regions of T_c where condition (32) is satisfied, then the approximation (33) applies. However at sufficiently low temperatures ($T_c < \tilde{J}/2$) we inevitably enter the other regime (38) where the asymptotics (30,31) change ($x < 1 \mapsto x > 1$), and the function $g(T_c)$ crosses over from (33) to (39). If, on the contrary, \tilde{J} is large, then condition (32) never applies, and the approximation (39) describes the whole region $T_c < 1/2$.

Extrema T_* of the function $g(T_c)$ (39) are determined by the transcendental equation

$$e^{-g_\lambda/2T_*} = \frac{\lambda\pi}{3g_\lambda\tilde{J}^2} T_*^3 \quad (40)$$

This equation always has a trivial solution $T_*' = 0$ corresponding to the (local) maximum of $g(T_c)$. This is the QCP, and the curve $T_c(g)$ approaches the QCP normally to the abscissa (see Fig. 8). Two non-trivial solutions of (40) exist if the couplings satisfy the condition

$$\tilde{J} > \mathbb{C}_1 \lambda^{\frac{1}{2}} g_\lambda, \quad (41)$$

where

$$\mathbb{C}_1 \equiv \sqrt{\frac{\pi}{24} \left(\frac{e}{3}\right)^3} \approx 0.3121. \quad (42)$$

There is only one solution within the validity region of the approximation (39), and it corresponds to the minimum of $g(T_c)$. If the couplings satisfy (41) then

$$u \equiv \ln 3 + \frac{1}{3} \ln a_o > 1 \quad (43)$$

$$a_o \equiv \frac{24\tilde{J}^2}{\pi\lambda g_\lambda^2},$$

and the minimum can be found analytically as

$$T_* \approx \frac{g\lambda}{6} \left(\frac{1}{u} - \frac{\ln u}{u^2} \right). \quad (44)$$

For the left border of the re-entrant region we obtain

$$g_{\min} = g\lambda - \frac{\lambda\pi}{3\tilde{J}^2} T_*^2 + \frac{4\lambda\pi}{3g\lambda\tilde{J}^2} T_*^3 \quad (45)$$

The above equations agree well with the numerical solutions of the MFA (21) at different values of couplings (from comparison of the asymptotics (33, 39) and the numerical curves at various couplings and temperatures we found the deviations $\sim 5\%$ at most). More importantly, the analytical results of this subsection allows us to understand in details the interplay of the scales provided by model's couplings and the temperature, resulting in the re-entrance. Let us explain this on the example of two characteristic numerical curves shown in Fig. 8.

The curve shown for $J = 0, \lambda = 1, \varepsilon = 0$ ($\tilde{J} = 0.25$) corresponds to the case of small \tilde{J} . At $T_c \gtrsim \tilde{J}/2 = 0.125$ it is well described by the equations for the regime (32). Its re-entrant behavior and, in particular, the minimum g_{\min} is due to the last term on the r.h.s. of (33). At lower temperatures $T_c \lesssim 0.125$ the asymptotics (33) is not applicable, the curve is described by (39). Note that since $\mathbb{C}_1 \lambda^{\frac{1}{2}} g_\lambda \approx 0.8229$, the condition (41) for the minimum is broken, and the asymptotics (39) describes the featureless low-temperature evolution of this curve towards the maximum at the QCP.

The second curve in Fig. 8 with $J = 0.75, \lambda = 1, \varepsilon = 0$ ($\tilde{J} = 1$) corresponds to the case of large \tilde{J} . The whole re-entrant region ($T_c < 0.4$), including the position of the minimum g_{\min} ($\mathbb{C}_1 \lambda^{\frac{1}{2}} g_\lambda \approx 0.8229$) is described by the interplay of the last two terms on the r.h.s. of Eq.(39). Comparison of Eqs.(36,45) allows also to understand a more pronounced re-entrant behavior for the case of smaller J .

As we see from our analysis of Eqs.(33,39) in the both regimes (32,38), the re-entrant behavior on the phase diagram occurs at any $\lambda \neq 0$.

2. Case $\varepsilon \neq 0$; double re-entrance, no QCP

The absence of re-entrance at $\lambda = 0$ can be proven rigorously. Indeed, combining Eqs.(28,29) we obtain the equation

$$m_z^{-1} = g + \frac{4\varepsilon^2}{\pi J} \eta_n \left(0, \frac{J}{2} \ln \frac{1 + 2m_z}{1 - 2m_z} \right) \quad (46)$$

which has one and only one solution $m_z \in [0, 1/2]$ for a given value of g . This solution in its turn provides a unique value of T_c via Eq.(29), thus no re-entrance.

At $\lambda \neq 0$ continuous evolution of $T_c(g)$ between the regimes of strong Ising coupling and BCS- [cf. Eq.(25)] can occur either with a double re-entrance [i.e., with one minimum and one maximum of $g(T_c)$] within the re-entrant region

$$g_{\min} < g < g_{\max}, \quad (47)$$

or without re-entrance. In the latter case the function $T_c(g)$ [or $g(T_c)$] has only an inflexion point (see Fig. 8).

Following the analysis given in the previous subsection, we obtain for the case of small \tilde{J} in the regime (32)

$$g = 2 + 4e^{-1/T_c} + \frac{\lambda\tilde{J} - 2\varepsilon^2}{4T_c} \quad (48)$$

Again, the re-entrant behavior is conditioned by the existence of a minimum of $g(T_c)$. It exists if, at least

$$\varepsilon < \frac{1}{\sqrt{2}} \sqrt{\lambda\tilde{J}} \approx 0.7071 \sqrt{\lambda\tilde{J}} \quad (49)$$

The unique minimum of $g(T_c)$ (48) defines the left border of the re-entrance region g_{\min} and corresponds to the critical temperature T_* given by Eqs.(35,36) with $\kappa_o \mapsto \kappa$, and

$$\kappa \equiv \frac{16}{\lambda\tilde{J} - 2\varepsilon^2} \quad (50)$$

The consistency imposes the constraint analogous to (37), more stringent than the “minimal requirement” (49).

The other regime (38) is described by the approximation

$$g = g_\lambda + 4e^{-g_\lambda/2T_c} - \frac{\pi T_c^2}{3\tilde{J}^3}(\lambda\tilde{J} + \varepsilon^2) - \frac{4\varepsilon^2}{\pi\tilde{J}} \ln \frac{\mathbb{A}\tilde{J}}{2T_c} \quad (51)$$

As we have explained in the previous subsection for the case $\varepsilon = 0$, the asymptotics (48) is applicable only for small \tilde{J} at the intermediate temperatures (32), while (51) can be applied at arbitrary low temperatures, including the BCS region. The latter, given by the exponential dependence in (25), can be recovered if we retain only the first and last (leading) terms on the r.h.s. of Eq.(51).

In the regime (38) the re-entrance occurs if the equation for extrema of (51)

$$e^{-g_\lambda/2T_*} = \frac{\pi T_*}{3g_\lambda \tilde{J}^3} \left[(\lambda\tilde{J} + \varepsilon^2) T_*^2 - \frac{6\varepsilon^2 \tilde{J}^2}{\pi^2} \right] \quad (52)$$

has non-trivial solutions. Note in making comparison of Eq.(52) to its counterpart (40) at $\varepsilon = 0$, that coupling ε destroys the QCP,⁶ as immediately seen from (51). So the trivial solution $T_* = 0$ of Eq.(52) corresponds to the unphysical singularity of g . As follows from (52,38), non-trivial solutions are possible if, at least

$$\varepsilon < \frac{\pi}{2\sqrt{6}} \frac{1}{\sqrt{1 - \frac{\pi^2}{24}}} \sqrt{\lambda\tilde{J}} \approx 0.8357 \sqrt{\lambda\tilde{J}} \quad (53)$$

If this condition is satisfied, the transcendental equation (52) has at least one solution, corresponding to maximum of $g(T_c)$. To leading order in ε , it occurs at the temperature

$$T'_* \approx \frac{\sqrt{6}}{\pi} \left(\frac{\tilde{J}}{\lambda} \right)^{\frac{1}{2}} \varepsilon \quad (54)$$

and the coupling

$$g_{\max} \approx g_\lambda - \frac{4\varepsilon^2}{\pi\tilde{J}} \ln \frac{\mathbb{A}\pi\sqrt{\lambda\tilde{J}}}{2\sqrt{6}\varepsilon} \quad (55)$$

If the couplings meet both the conditions (41) and

$$\varepsilon < \mathbb{C}_2 g_\lambda \left(\frac{\lambda}{\tilde{J}} \right)^{\frac{1}{2}}, \quad (56)$$

where

$$\mathbb{C}_2 \equiv \frac{\pi}{2} \sqrt{\frac{47 - 13\sqrt{13}}{36}} \approx 0.0936, \quad (57)$$

then a second solution of (52) (T''_*), corresponding to minimum of $g(T_c)$ exists. This minimum, located between

$$T'_* < T''_* < \frac{g_\lambda}{6} \quad (58)$$

is given approximately by Eq.(44) where u in (43) is modified by $a_o \mapsto a$, and

$$a \equiv \frac{24\tilde{J}^3}{\pi g_\lambda^2 (\lambda\tilde{J} + \varepsilon^2)} \quad (59)$$

For validity of expansion (44) we assume $u > 1$.

The analytical results of this subsection allows us to describe the behavior of the coupled model at $\varepsilon \neq 0$, following from the MFA equations (21), both qualitatively and quantitatively. In Fig. 8 two counterparts ($\varepsilon = 0.1$) of the numerical curves discussed in the previous subsection are shown. For this case of small ε , re-entrance is possible, according to conditions (49,53). The re-entrant behavior at the temperatures $T_c \gtrsim T'_*$ is not modified essentially by the presence of new coupling ε comparatively to the case $\varepsilon = 0$, and is in fact controlled by couplings J, λ, g . Since we have already discussed it in detail for the case $\varepsilon = 0$, we will not dwell on it any more. In the low-temperature

regime (51) coupling ε changes drastically the behavior of $g(T_c)$ at $T_c \lesssim T'_*$, creating a maximum at $g(T'_*)$ described well by the approximation (54) and turning $g(T_c)$ away from the QCP towards the BCS region. For the BCS regime Eq.(25) provides a virtually exact solution.

As follows from the inequalities (49,53,56) an increase of ε can suppress the re-entrance even at $\lambda \neq 0$. The necessary conditions (49,53) for extrema of the two asymptotics (48,51) are close, albeit with a rather small mismatch of the coefficient. Conditions for re-entrance are more stringent, since they require the consistency between the solutions for extrema and the validity ranges of the appropriate asymptotics. The (overrated) critical value $\varepsilon_o \sim 0.7\sqrt{\lambda\tilde{J}}$ gives a good simple estimate for the boundary where the re-entrance disappears from the whole curve $g(T_c)$, whether $\tilde{J} > 1$ or $\tilde{J} < 1$. An example of the curve $T_c(g)$ without re-entrance is shown in Fig. 8.

To summarize our analysis of the re-entrance for the cases $\varepsilon = 0$ and $\varepsilon \neq 0$: it reveals the robustness of this phenomenon in the coupled model (14) and its underlying mechanism, namely, competition between different scales defined by the couplings $J, \lambda, \varepsilon, g$ and the temperature. Note that these competing scales (interactions) are not related to the Ising frustration which is present in the model as well [$(J_\square, J_1, J_2) > 0$], since the latter is not accounted for explicitly by our mean-field equations. This competing mechanism for the re-entrance appears to be robust and not being an artifact of the MFA. Note that a re-entrance due to competing interactions was found even from the exact solution of the Ising model on the union-jack lattice.³⁰

IV. CONCLUSIONS

We study the 2D Ising model on a square lattice with nearest-neighbor (nn) and next-nearest neighbor (nnn) interactions for the case of equal nn couplings J_\square and arbitrary nnn diagonal couplings J_1, J_2 . The cases of classical ($\Omega = 0$) and quantum ($\Omega \neq 0$) models, where Ω is a transverse field, are considered. In a particular region of (J_\square, J_1, J_2) corresponding to the Ising model's super-antiferromagnetic (SAF) ground state, we analyze the coupled spin-pseudospin model, comprised of the quantum Ising model coupled to XY spin chains.

We find the ground state phase diagram of the classical Ising model at arbitrary J_\square, J_1, J_2 . Along with the three ordered phases—ferromagnetic (FM), antiferromagnetic (AF), and SAF—known for the case $J_1 = J_2$,⁸ in the case when $J_1 \neq J_2$ we find a region of the coupling space with the super-ferro-antiferromagnetic (SFAF) [or (4×4)] ground state phase, and an incommensurate (IC) phase at finite temperature. The three phases – SAF, SFAF, IC – can occur only in the presence of competing interactions (frustrations) on the Ising model's plaquette.

Combining the mapping of the quantum model at $T = 0$ onto its classical 3D counterpart with the mean-field arguments, we locate the ground-state phase boundaries of the quantum model in the coupling space (J_\square, J_1, J_2) . A particularly interesting conclusion of this analysis is that the transverse field can cause the IC ground-state phase, located at $\Omega = 0$ completely in a quite “exotic” region $sign(J_1/J_2) = -1$, into some parts of, e.g., the AF and SAF regions of the coupling space where $(J_1, J_2) > 0$, but $J_1 \neq J_2$. These regions, along with proximities of the special (triangulation and frustration) planes of degeneracy in the coupling space, are good candidates for the quantum model to demonstrate a very non-trivial critical behavior. Leaving this for a future work, we hope that our findings would inspire some interest in this model. Taking into account only one simple example of a mapping shown in Fig. 7, it is clear that nnn model with $J_1 \neq J_2$ is not so exotic.²⁶

The present study of the nn and nnn IMTF coupled to the XY spin chains is restricted to the SAF region of (J_\square, J_1, J_2) , where the IMTF has a simple two-phase (disordered-SAF) diagram with a QCP, similar to that of the transverse nn model. We studied earlier⁶ a similar coupled model in the context of the quasi-2D ladder compound NaV_2O_5 . The mean-field equations of Ref.[6] and their predictions for the model's phase diagram are the same, up to some coupling's modifications. However in the present work we gain more insights on the spin-SAF transition in this spin-pseudospin model and sharpen our previous statements concerning the applications to NaV_2O_5 .

The present analysis of Ising's sector of the coupled model allows us for the first time to identify the 2D long-range charge order in that compound as the SAF phase. From the known facts on the ordering into the SAF phase,¹ this leads to a conclusion that the transition in NaV_2O_5 has non-universal coupling-dependent critical indices. However, since in the limit $J_\square \rightarrow 0$ the PM-SAF transition enters into the 2D Ising universality class, and for NaV_2O_5 the ratio $J_\square/J_1 < 1$ (at least), in practice the deviations from the universality should be rather small. Experiments give $\beta \approx 0.17 - 0.19$,^{31,32,33} which is close to $\beta = 1/8$ of the 2D Ising model. Due to known difficulties in extracting critical indices from experimental data, it seems unlikely to diagnose the deviations from universality caused by $0 < J_\square/J_1 < 1$.

On the theory side, the critical indices of the PM-SAF transition as coupling's functions have been calculated within various methods only at $J_1 = J_2$,¹ while for the case of non-equal diagonal couplings they are unknown. It appears to be a very interesting problem to analyze the critical indices of the latter case, and especially at $J_2 \ll J_1$ for the SAF regime of couplings, since in the limit $J_2 \rightarrow 0$ the nn and nnn model crosses over to the (disordered at any $T > 0$, but quantum critical) anisotropic triangular Ising model.

The predictions of the mean-field equations for the critical properties of the coupled spin-pseudospin model do not differ from our earlier results for a simpler Hamiltonian.⁶ Due to the nnn spin-pseudospin coupling ε the QCP of the nn and nnn IMTF is destroyed, and in the all considered SAF region of Ising couplings the spin-pseudospin model undergoes the spin-SAF transition. We should point out, that albeit the exponential BCS regime (25) on the disordered side of the IMTF QCP $g < g_\lambda$ formally extends up to $g = 0$, decreasing g , i.e. $J_1 + J_2$, will eventually remove us from the coupling region (11) where the MFA equations with the SAF pseudospin solution are applicable.

In this paper we perform a detailed analytical study of re-entrance in the coupled model. In particular, we establish the conditions when it can occur. The analytical results not only agree well with the direct numerical calculations in various regimes, but allows us to understand the physical mechanism of re-entrance due to interplay of competing interactions in the coupled model.

Acknowledgments

We are grateful to D.I. Khomskii, E. Orignac, and P.N. Timonin for helpful discussions. This work is supported by the German Science Foundation.

-
- ¹ R. Liebmann, *Statistical Mechanics of Periodic Frustrated Ising Systems* (Springer, Berlin, 1986).
- ² We use the term “frustrated” in a broad sense,¹ meaning only that there is no spin arrangement on an elementary plaquette which can satisfy all bonds.
- ³ B.K. Chakrabarti, A. Dutta, and P. Sen, *Quantum Ising Phases and Transitions in Transverse Ising Models* (Springer, Berlin, 1996).
- ⁴ R. Moessner and S.L. Sondhi, Phys. Rev. B **63**, 224401 (2001).
- ⁵ M.V. Mostovoy, D.I. Khomskii, J.Knoester, and N.V. Prokof'ev, Phys. Rev. Lett. **90**, 147203 (2003).
- ⁶ G.Y. Chitov and C. Gros, cond-mat/0310494.
- ⁷ P. Lemmens, G. Güntherodt, and C. Gros, Phys. Reports. **375**, 1 (2003).
- ⁸ C. Fan and F.Y. Wu, Phys. Rev. **179**, 560 (1969).
- ⁹ Such state, with the name of (4×4) superstructure was described before, e.g., by D.P. Landau and K. Binder, Phys. Rev. B **31**, 5946 (1985). It can occur in the 2D Ising model where along with nn and nnn, the third-neighbor interactions are included.
- ¹⁰ P. Bak, Rep. Prog. Phys. **45**, 587 (1982).
- ¹¹ W. Selke, Phys. Rep. **170**, 213 (1988).
- ¹² S. Krinsky and D. Mukamel, Phys. Rev. B **16**, 2313 (1977).
- ¹³ E. Domany, M. Schick, J.S. Walker, and R.B. Griffiths, Phys. Rev. B **18**, 2209 (1978).
- ¹⁴ G.H. Wannier, Phys. Rev. **79**, 357 (1950); Errata: Phys. Rev. B **7**, 5017 (1973).
- ¹⁵ R.M.F. Houtappel, Physica **16**, 425 (1950).
- ¹⁶ J. Stephenson, J. Math. Phys. **11**, 413 (1970).
- ¹⁷ J. Stephenson, J. Math. Phys. **11**, 420 (1970).
- ¹⁸ The well studied ANNNI phase diagram with the FM and antiphase ground states (see Refs.[1,10,11] for review) is an analogue of the lower part of the fourth quadrant (FM-SFAF) of our diagram in Fig. 2.
- ¹⁹ According to this notation, the antiphase of the 2D ANNNI model is (1×4) . For the same reasons we give for our case, the floating phase of that model exists only within the antiphase ground-state region.
- ²⁰ S.N. Coppersmith, D.S. Fisher, B.I. Halperin, P.A. Lee, and W.F. Brinkman, Phys. Rev. B **25**, 349 (1982); Phys. Rev. Lett. **46**, 549 (1981); Erratum: Phys. Rev. Lett. **46**, 869 (1981).
- ²¹ By analogy with the triangular Ising case of Refs.[4,5], we expect the transverse field to bring about new exotic phases near the frustration planes FP, FP', where the ground state of the model is also highly degenerate.
- ²² K.I. Kugel and D.I. Khomskii, Usp. Fiz. Nauk **136**, 621 (1982); [Sov. Phys. Usp. **25**(4), 231 (1982)].
- ²³ M.V. Mostovoy and D.I. Khomskii, Solid St. Comm. **113**, 159 (1999); cond-mat/9806215.
- ²⁴ D. Sa, C. Gros, Eur. Phys. J. B **18**, 421 (2000).
- ²⁵ M.V. Mostovoy, D.I. Khomskii, and J. Knoester, Phys. Rev. B **65**, 064412 (2002).
- ²⁶ Note that a linear coupling $\propto \varphi(\mathcal{T}_1 \mp \mathcal{T}_2)$ with some Gaussian mode φ results in an effective anti-/ferro-magnetic interaction between \mathcal{T}_1 and \mathcal{T}_1 . Such terms can create or renormalize the couplings of the Ising effective Hamiltonian. From this point of view, e.g., the considered above case of the Ising model with two diagonals of different signs seems to be less academic than it might appear.
- ²⁷ Since in applications to NaV_2O_5 we associate the pseudospins \mathcal{T} of the Ising model with charge displacements, we will call the disordered phase “paraelectric” (PE) and the ordered one “super-antiferroelectric”, keeping however the same abbreviation SAF for the latter.
- ²⁸ This type of coupling is allowed by the symmetry of the original NaV_2O_5 lattice.⁶
- ²⁹ R. Blinc and B. Žekš, *Soft Modes in Ferroelectrics and Antiferroelectrics*, (North-Holland Publishing Co., Amsterdam, 1974).

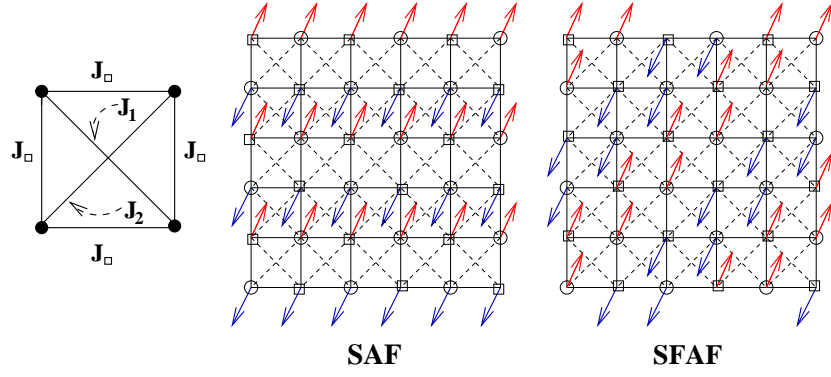


FIG. 1: Left: Couplings on an elementary plaquette in the nn and nnn 2D Ising model (1). Spin ordering in the super-antiferromagnetic (SAF) and super-ferro-antiferromagnetic (SFAF) phases.

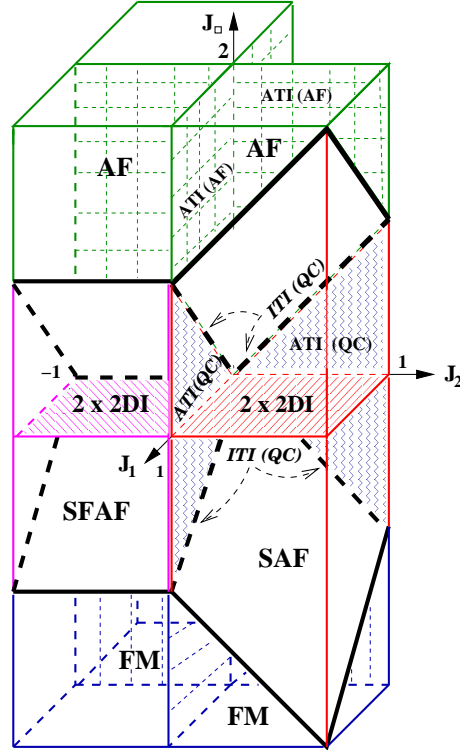


FIG. 2: Phase diagram of the ground states (GS) of the model (1). For visualization purposes it is drawn within $(-1, 1) \times (-1, 1) \times (-2, 2)$ parallelepiped. The SAF GS (red, online) lies between the frustration planes $J_1 + J_2 = |J_\square|$ (bold black). The SFAF GS (magenta, online) lies between the frustration planes $J_1 = |J_\square|$ (bold black). The AF GS, green, online (FM GS, blue, online) lies above (beneath) the frustration planes and above (beneath) the basal plane in the third quadrant, respectively. The second quadrant (not shown) is obtained by a reflection over $J_1 = J_2$ plane. Different sectors shown by hatched and twiggly lines on the exactly-solvable planes $J_\square = 0$ are explained in the text.

³⁰ V.G. Vaks, A.I. Larkin, and Y.N. Ovchinnikov, Zh. Eksp. Teor. Fiz. **49**, 1180 (1965) [Sov. Phys. JETP, **22**, 820 (1966)].

³¹ S. Ravy, J. Jegoudez, and A. Revcolevschi, Phys. Rev. B **59**, 681 (1999).

³² B.D. Gaulin, M.D. Lumsden, R.K. Kremer, M.A. Lumsden, and H. Dabkowska, Phys. Rev. Lett. **84**, 3446 (2000).

³³ Y. Fagot-Revurat, M. Mehring, and R.K. Kremer, Phys. Rev. Lett. **84**, 4176 (2000).

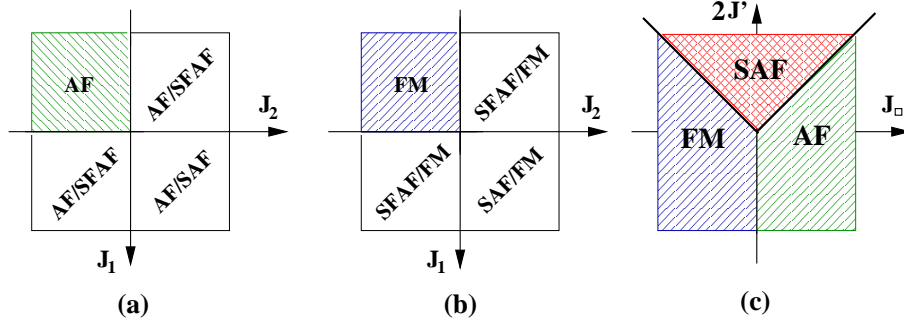


FIG. 3: Plane projections of the 3D diagram shown in Fig. 2. (a): Upper part $J_\square > 0$, view from the top. (b): Lower part $J_\square < 0$, view from the top. (c): Compactification of 3D Fig. 2 in the special case $J_1 = J_2 \equiv J'$ (Ref.[8]).

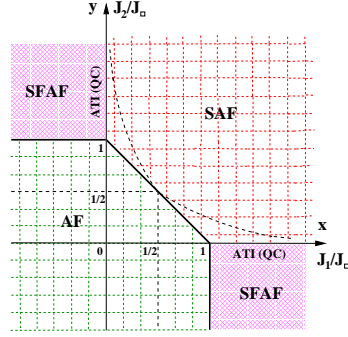


FIG. 4: Plane phase diagram for the ratios of the couplings, corresponding to the 3D Fig. 2 at $J_\square > 0$. The phase boundaries (thick solid lines) correspond to the frustration planes FP and FP'. The thick dashed lines (black, online) indicate the boundaries of the incommensurate global minima locus ($y > 1/2$, $x > 1/2$, $y < 1/4x$) discussed in the text. The case $J_\square < 0$ can be obtained by the substitutions $J_{1,2}/J_\square \mapsto J_{1,2}/|J_\square|$, AF \mapsto FM in this figure.

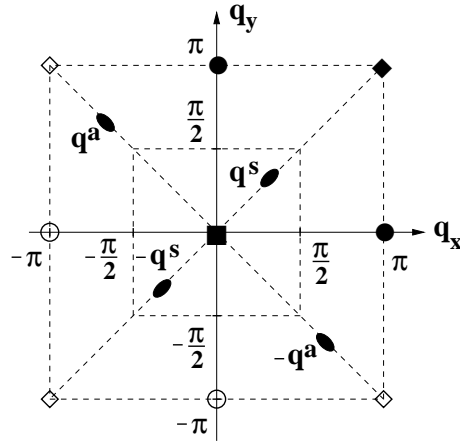


FIG. 5: Positions of extrema of $J(\mathbf{q})$ (5) in the Brillouin zone. Open symbols connected to their bold counterparts by a reciprocal lattice vector. Incommensurate extrema $\pm \mathbf{q}^{a,s}$ (7,8) (shown for the case $J_1 > 0$, $J_2 < 0$) exist if conditions (6) are satisfied.

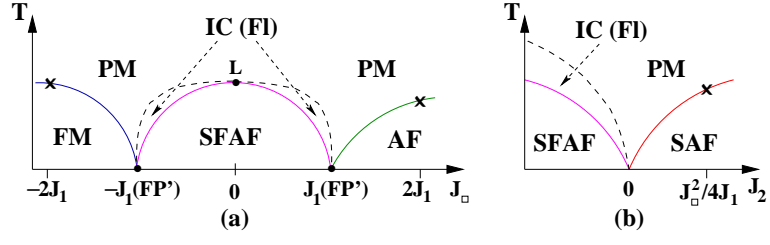


FIG. 6: Qualitative temperature phase diagram. The IC floating [IC (FI)] phase lies beneath the dashed lines. Crosses indicate the borders of the IC minima locus. (a): For fixed $J_1 > 0$, $J_2 < 0$. On the plane $J_\square = 0$ the floating phase must be absent. We assume that it smoothly disappears at $J_\square = 0$ resulting in a Lifshitz point (L). (b): The same for fixed $J_1 > 0$, $|J_\square| < J_1$.

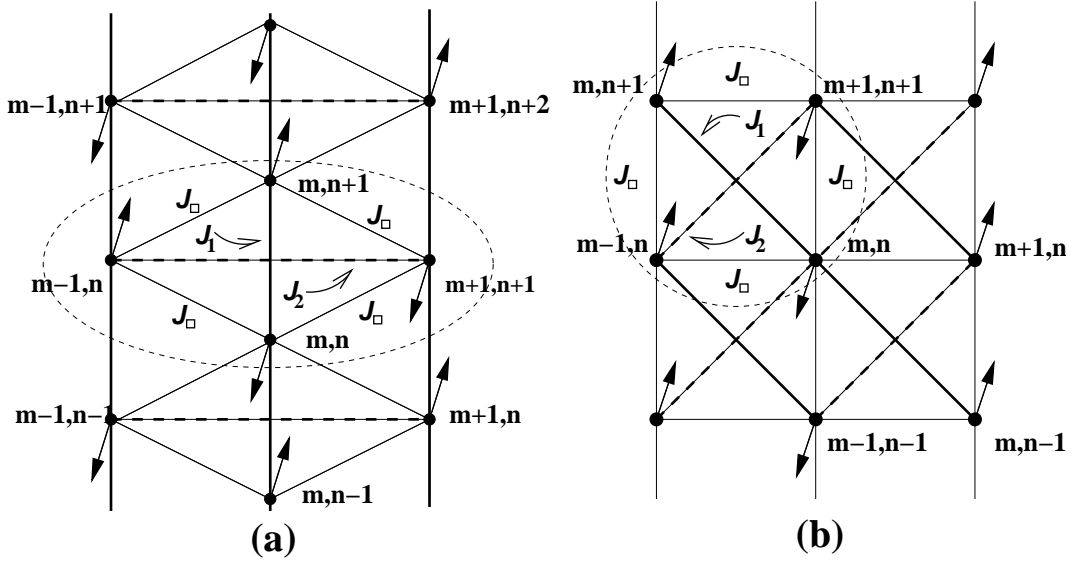


FIG. 7: (a): Two-dimensional “effective” lattice of coupled ladders. A vertical line denotes a single ladder where a dot denotes its rung. At each rung (m, n) there is pseudospin \mathcal{T}_{mn} and spin \mathbf{S}_{mn} (not shown). In the region encircled by the dashed line we indicate the Ising couplings between neighboring pseudospins. Two pseudospins from $(m-1)$ -th and $(m+1)$ -th ladders are coupled not only by J_2 (bold dashed line), but also via the dimerization interaction constant ε . The pseudospin \mathcal{T}_{mn}^x ordering pattern shown in the figure corresponds to the ordered SAF phase. (b): The same after mapping on a square lattice.

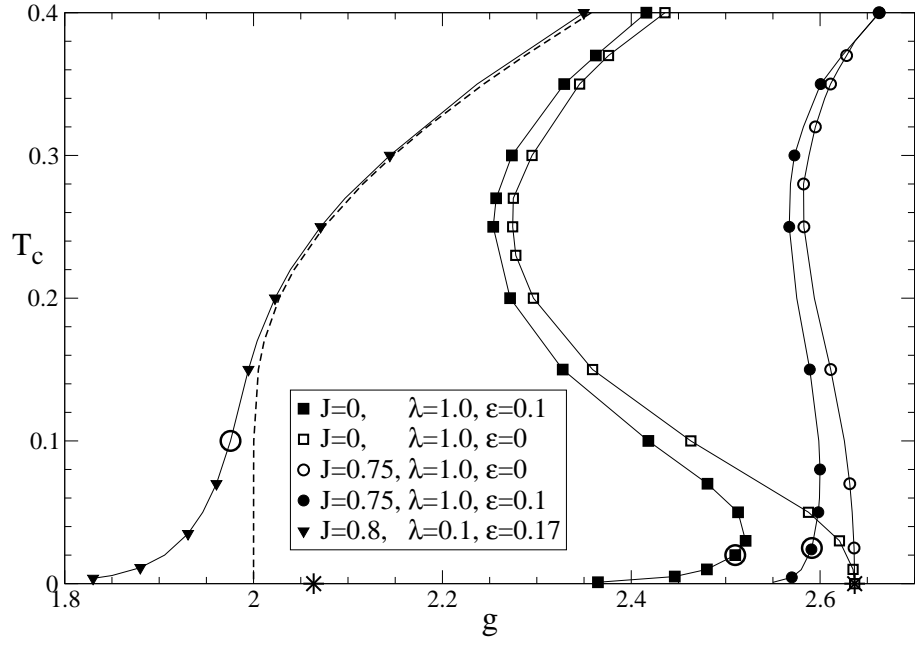


FIG. 8: Critical temperature of the PE-SAF phase transition as a function of the Ising coupling g at different values of J, λ, ε from the numerical solution of Eqs.(21). The dashed line corresponds to the pure IMTF ($J = \lambda = \varepsilon = 0$). Two stars on the abscissa show the positions of critical couplings $g_\lambda = 2.0627$ (2.6366) for $\lambda = 0.1$ (1.0), resp. Large empty circles on the curves with $\varepsilon \neq 0$ indicate the right boundary of the exponential BCS regime (25). At large values of g (not shown) all curves $T_c(g)$ approach the asymptotic line $T_c = g/4$.